(*A*.9) becomes

$$I_v(\tau) \simeq C_1 V \int \mathrm{d}\mathbf{u}_b \int \mathrm{d}\mathbf{u}'_b \int_0^\infty \mathrm{d}\omega (1/u'^2) \times \mathrm{Im}\{-[1/\varepsilon_{\mathbf{u}\mathbf{u}'}(\omega)] Z(\boldsymbol{\tau}-\mathbf{u}_b, \omega) \times Z^*(\boldsymbol{\tau}-\mathbf{u}'_b, \omega)\}, \quad (A.10)$$

where $C_1 = e^2 m_0^2/\pi\varepsilon_0\hbar^3$. Equation (*A*.10) is a generalized intensity distribution in the valence-loss electron diffraction pattern. Now consider a case where the dielectric function depends only on the electron energy loss, for a homogeneous medium

$$1/\varepsilon_{\tau\tau'}(\omega) = [1/\varepsilon(\omega, \boldsymbol{\tau})]\delta(\boldsymbol{\tau}-\boldsymbol{\tau}')\delta(\tau_z - q_n). \quad (A.11)$$

Thus (*A*.10) becomes

$$\begin{aligned} I_v(\tau) &= (e^2 k_0^2 V_s/\pi\varepsilon_0 v^2) \int_0^\infty \mathrm{d}\omega \int \mathrm{d}\mathbf{u}_b (u_b^2 + q_n^2)^{-1} \\ &\quad \times \mathrm{Im}[-1/\varepsilon(\omega, \mathbf{u}_b)] |Z(\boldsymbol{\tau}-\mathbf{u}_b, \omega)|^2 \\ &= (e^2 k_0^2 V_s/\pi\varepsilon_0 v^2) \int_0^\infty \mathrm{d}\omega \{(\tau^2 + q_n^2)^{-1} \\ &\quad \times \mathrm{Im}[-1/\varepsilon(\omega, \boldsymbol{\tau})]\} \otimes |Z(\boldsymbol{\tau}, \omega)|^2. \quad (A.12) \end{aligned}$$

Therefore, the diffraction pattern is composed of the incoherent addition of all the electrons with different energy losses $\hbar\omega$ and momentum transfers, weighted by the probability functions. For the energy-filtered diffraction patterns of a narrow energy window, the integration of energy in (*A*.12) is dropped. It is important to note that (*A*.12) has the same form as (10) for localized inelastic scattering, thus the corresponding T function can be readily written as (23).

References

BIRD, D. M. & WRIGHT, A. G. (1989). *Acta Cryst.* A**45**, 104-109.
BORN, M. (1942). *Rep. Prog. Phys.* **9**, 294-333.
COWLEY, J. M. (1988). *Acta Cryst.* A**44**, 847-855.
COWLEY, J. M. & MOODIE, A. F. (1957). *Acta Cryst.* **10**, 609-619.
DOYLE, P. A. (1970). *Acta Cryst.* A**26**, 133-139.
EGERTON, R. F. (1986). *Electron Energy-Loss Spectroscopy in Electron Microscopes*. New York: Plenum Press.
FANIDIS, C., VAN DYCK, D., COENE, W. & VAN LANDUYT, J. (1989). In *Computer Simulation of Electron Microscope Diffraction and Images*, edited by W. KRAKOW & M. O'KEEFE, pp. 135-158. London: The Minerals, Metals and Materials Society.
GJØNNES, J. (1966). *Acta Cryst.* **20**, 240-249.
GJØNNES, J. & WATANABE, D. (1966). *Acta Cryst.* **21**, 297-302.
HALL, C. R. & HIRSCH, P. B. (1965). *Proc. R. Soc. London Ser. A*, **286**, 158-177.
HØIER, R. (1973). *Acta Cryst.* A**29**, 663-672.
HOWIE, A. (1963). *Proc. R. Soc. London*, **271**, 268-287.
ISHIZUKA, K. (1982). *Acta Cryst.* A**38**, 773-779.
ISHIZUKA, K. & UYEDA, N. (1977). *Acta Cryst.* A**33**, 740-749.
KOHL, K. & ROSE, H. (1985). *Adv. Electron. Electron Phys.* **65**, 173-227.
LOANE, R. F., XU, P. & SILCOX, J. (1991). *Acta Cryst.* A**47**, 267-278.
PALIK, E. D. (1985). Editor. *Handbook of Optical Constants of Solids*. New York: Academic Press.
REIMER, L., FROMM, I. & NAUNDORF, I. (1990). *Ultramicroscopy*, **32**, 80-91.
REZ, P., HUMPHREYS, C. J. & WHELAN, M. J. (1977). *Philos. Mag.* **35**, 81-96.
ROSSOUW, C. J. (1985). *Ultramicroscopy*, **16**, 241-254.
ROSSOUW, C. J. & BURSILL, L. A. (1985). *Acta Cryst.* A**41**, 320-328.
SELF, P. & O'KEEFE, M. (1989). In *High-Resolution Transmission Electron Microscopy and Associated Techniques*, edited by J. M. COWLEY, P. BUSECK & L. EYRING, pp. 244-307. New York: Oxford Univ. Press.
WANG, Z. L. (1990). *Phys. Rev. B*, **41**, 12818-12836.
WANG, Z. L. (1991). *Acta Cryst.* A**47**, 686-698.
WANG, Z. L. (1992). *Philos. Mag.* B**65**, 559-587.
WANG, Z. L. & BENTLEY, J. (1991*a*). *Ultramicroscopy*, **38**, 181-213.
WANG, Z. L. & BENTLEY, J. (1991*b*). *Microsc. Microstruct. Microanal.* **2**, 301-314.
WANG, Z. L. & BENTLEY, J. (1991*c*). *Inst. Phys. Conf. Proc.* No. 119, pp. 547-550.
WANG, Z. L. & BENTLEY, J. (1991*d*). *Microsc. Microstruct. Microanal.* In the press.
WANG, Z. L. & BENTLEY, J. (1991*e*). In *Proc. 49th Annu. Meet. Electron Microsc. Soc. Am. (San Jose)*, edited by G. W. BAILEY & E. L. HALL, pp. 708-709. San Francisco Press.
WHELAN, M. J. (1965*a*). *J. Appl. Phys.* **36**, 2099-2103.
WHELAN, M. J. (1965*b*). *J. Appl. Phys.* **36**, 2103-2110.
YOSHIOKA, H. (1957). *J. Phys. Soc. Jpn*, **12**, 618-628.

Acta Cryst. (1992). A**48**, 688-692

Resolution Investigations of X-ray Three-Crystal Diffractometers

BY L. BRÜGEMANN, R. BLOCH, W. PRESS AND M. TOLAN

Institut für Experimentalphysik, Universität Kiel, Leibnizstrasse 19, *D*-2300 *Kiel* 1, *Germany*

(*Received* 10 *August* 1991; *accepted* 6 *March* 1992)

Abstract

The object of this study is the resolution of a three-crystal diffractometer (TCD) using perfect crystals as monochromator and analyser. It relates to the resolution as a function of the scattering vector **Q**. This information is crucial for the interpretation of high-resolution X-ray diffraction data obtained very close to reciprocal-lattice points. In this light we present the experimentally determined resolution of TCDs

0108-7673/92/050688-05$06.00

using silicon 111 as well as germanium 111 and 311 reflections, respectively. The values are compared with calculations based on recently published models.

1. Introduction

High-brilliance X-ray sources, such as rotating anodes, or synchrotron-radiation sources have opened the way to obtaining experimental resolutions in the range of $\delta q \sim 10^{-4}$ Å^{-1}. These experiments were mostly performed with three-crystal diffractometers (TCDs) using perfect monochromator and analyser crystals. Problems such as crystal truncation rods (CTRs) due to the termination of the bulk lattice by its surface (Robinson, 1986; Robinson, Waskiewicz, Tung & Bohr, 1986), Bragg-like scattering from superlattices (Ryan, Hatton, Bates, Watt, Sotomeyer-Torres, Claxton & Roberts, 1987) or Bragg and diffuse scattering near phase transitions (Ryan, 1986) are objects of high-resolution X-ray diffraction studies. For the interpretation of such data it is necessary to know the resolution function $R(\mathbf{Q}-\mathbf{Q}_0)$. We choose the following notation in this paper. The scattering plane is defined by the x and y directions; z components of vectors are out of plane. $\mathbf{Q}=\mathbf{k}_f-\mathbf{k}_i$ denotes the momentum transfer between the wave vectors $\mathbf{k}_i$ and $\mathbf{k}_f$ of the incident and diffracted X-ray beams. The nominal setting of the instrument is $\mathbf{Q}_0$. The diffracted intensity $I(\mathbf{Q}_0)$ can be obtained by a convolution (*) of the resolution function $R(\mathbf{Q}-\mathbf{Q}_0)$ and the scattering function $S(\mathbf{Q})$:

$$I(\mathbf{Q}_0)=R*S=\int R(\mathbf{Q}-\mathbf{Q}_0)S(\mathbf{Q})\,\mathrm{d}\mathbf{Q}. \quad (1)$$

The deviation of $\mathbf{Q}$ from the nominal scattering vector of the instrument $\mathbf{Q}_0$ is called $\Delta\mathbf{Q}$ ($\mathbf{Q}=\mathbf{Q}_0+\Delta\mathbf{Q}$).

In this paper we distinguish between two different ranges of the resolution of a given TCD.

1. In the central part of the resolution function, *i.e.* the region of high intensities, a Gaussian approximation is appropriate and the resolution is characterized by the full width at half-maximum (FWHM).

2. In experiments that cover a large range of intensities, details of the scattering become visible, which include the surfaces of the crystals involved (later on we call this 'star-like resolution').

Several authors have calculated the resolution function for a neutron three-crystal spectrometer (Cooper & Nathans, 1967; Chesser & Axe, 1973; Grimm, 1984). In the case of an X-ray diffractometer using perfect monochromator and analyser crystals, the calculation of the resolution function is somewhat more complicated because dynamical scattering effects have to be considered. Nevertheless, the central part of the resolution function could be calculated with the help of treatments initially introduced by Cooper & Nathans (1967) for neutron diffraction. This was done by Cowley (1987), but without comparing his results with measurements. A more complex treatment was used by Pynn, Fujii & Shirane (1983). The star-like resolution was first shown by Iida & Kohra (1979) and later calculated by Zaumseil & Winter (1982). A quantitative comparison between measurement and calculation is still lacking, however.

In this paper, we present the calculated and measured resolution function $R(\mathbf{Q}-\mathbf{Q}_0)$ for X-ray TCDs with perfect silicon and germanium crystals. The central part was calculated following the treatment of Cowley, whereas the star-like resolution was treated in the spirit of the procedure published by Zaumseil & Winter (1982).

2. Theoretical treatment

A thorough description of the central part of the resolution function $R(\mathbf{Q}-\mathbf{Q}_0)$ is given by Cowley (1987), the main ideas originating from Cooper & Nathans (1967). By considering the elastic scattering only and by treating the out-of-plane resolution δq_z as decoupled from the resolution of the TCD in the scattering plane, one obtains, in a Gaussian approximation for the resolution function,

$$R(\mathbf{Q}-\mathbf{Q}_0)=R_0\exp\{-0.5(M_{11}\,\Delta Q_x^2 + 2M_{12}\,\Delta Q_x\,\Delta Q_y + M_{22}\,\Delta Q_y^2)\}. \quad (2)$$

ΔQ_x and ΔQ_y are the components of $\mathbf{Q}-\mathbf{Q}_0$ parallel and perpendicular to the nominal scattering vector $\mathbf{Q}_0$ within the scattering plane. Both ΔQ_x and ΔQ_y are functions of $|\mathbf{Q}_0|$. The matrix elements $M_{ij}(\mathbf{Q}_0)$ can be evaluated for various diffractometer configurations and R_0 is a scale factor.

The Gaussian approximation will lead to reasonable results as long as the tails of the Darwin profile need not be taken into account. Furthermore, the assumption $|\Delta\mathbf{Q}| \ll |\mathbf{Q}_0|$ has to be fulfilled (Cooper & Nathans, 1967).

By using the same Bragg reflection for the monochromator and the analyser (here silicon 111), the mixed term in the exponent of (2) vanishes and the exponent can be seen as an equation for an ellipsoid transformed to main axes,

$$M_{11}\Delta Q_x^2+M_{22}\Delta Q_y^2=2C. \quad (3)$$

For $C=$ constant, (3) describes ellipsoidal isointensity contours. The full width at half-maximum (FWHM) of the intensity defines the resolution δq. From (2) one obtains $\delta q_x=(8\ln 2/M_{11})^{1/2}$ (resolution parallel to $\mathbf{Q}_0$) and $\delta q_y=(8\ln 2/M_{22})^{1/2}$ (in-plane resolution perpendicular to $\mathbf{Q}_0$).

To interpret the measured intensity distribution for a wide dynamical range at a large distance from a reciprocal-lattice point one has to consider the influence of the tails of the Darwin profiles of the monochromator, analyser and sample-crystal reflections. For perfect crystals, a star-like intensity

distribution will appear (Iida & Kohra, 1979). Apart from the intensity streak originating from the tails of the Darwin profiles of the perfect sample crystal, two further streaks are visible. They intersect the CTR of the sample with the Bragg angle $\pm\Theta_{\mathrm{Bragg}}$ of the investigated reflection. Note that the tails of the Darwin profiles and the so-called crystal truncation rods (CTRs), introduced by Robinson (1986), are only two different descriptions of the same fact.

The detailed shape of the resolution function can be determined both theoretically and experimentally by taking an ideal crystal as the sample and using the Bragg reflection of a reciprocal-lattice point $\mathbf{G}_{hkl}$ [$|\mathbf{G}_{hkl}| = 2\pi/d(hkl)$, where $d(hkl)$ is the lattice spacing of the (hkl) planes] for sampling the resolution. In principle, a small error is made using this procedure because convolution with the δ function $\delta(\mathbf{Q}-\mathbf{G}_{hkl})$ would be necessary to obtain the resolution function directly [see (1)]. In our case the scattering function $S(\mathbf{Q})$ itself has a Darwin width, which adds to the width of the measured resolution function.

The intensity distribution $I(\Delta Q_x, \Delta Q_y)$ can be calculated near a reciprocal-lattice point following the description given by Pinsker (1978) and as calculated by Zaumseil & Winter (1982) in a similar way. Two successive convolutions (*) need to be performed to calculate $I(\Delta Q_x, \Delta Q_y)$:

$$I(\Delta Q_x, \Delta Q_y) = (C_M * C_S) * C_A = \int (C_M * C_A) S(\mathbf{Q})\, \mathrm{d}\mathbf{Q}. \quad (4)$$

Here the C_i represent the Bragg-reflection curves of the crystals and $\Delta\mathbf{Q} = \mathbf{Q} - \mathbf{G}_{hkl}$ is the deviation from the reciprocal-lattice point. $C_S = S(\mathbf{Q})$ describes the scattering law of the investigated Bragg reflection and $R = C_M * C_A$ is the resolution function [see (1)] of the diffractometer. For stronger departures from the exact Bragg position, the intensity reflected from a single crystal with a plane surface decreases as ΔQ_x^{-2}. If ΔQ_x is smaller than the Darwin width of the reflection, a reflectivity near 1 will be taken. In this approximation, absorption effects are neglected. Calculated and measured results are shown below.

3. Results

Below we compare the calculations with experimental data. For this purpose we used TCDs with two types of perfect monochromator and analyser crystals. First, we used silicon 111 reflections for both crystals and, second, we performed the resolution experiments with germanium 111 and 311 reflections, respectively. The experimental set-up for both types of investigation is shown in Fig. 1. To measure the intensity distribution around a reciprocal-lattice point (*i.e.* the resolution) for different values of $\mathbf{Q}_0$, we took as samples Si 111 (Brügemann, Bloch, Press & Gerlach, 1990), GaAs 004 (Bloch, Bahr, Olde, Brügemann & Press, 1990) and, in the range of small $|\mathbf{Q}_0|$, a thick amorphous germanium layer on silicon (Bloch, Brügemann & Press, 1989).

As an X-ray source, Cu $K\alpha_1$ radiation from a rotating-anode tube was used. The intrinsic line width $\Delta\lambda/\lambda$ was 4.8×10^{-4} at a wavelength of $\lambda = 1.54056$ Å. The full Darwin width for the Si 111 reflection was taken as 33.6 μrad, whereas it was 84.2 μrad and 39.2 μrad for Ge 111 and 311. The experimental resolutions $\delta q_x(|\mathbf{Q}_0|)$ and $\delta q_y(|\mathbf{Q}_0|)$ were obtained by fitting Gaussians to the measured data. Then they are given as the FWHM of the fitted curves. The data collection was done by rotating the sample at fixed scattering angle (rocking curve). In reciprocal space this is a ΔQ_y scan at fixed ΔQ_x (for small ΔQ_y). A set of rocking curves yielded an intensity distribution around each reciprocal-lattice point. In this way a complete picture of the resolution ellipsoid was acquired. A cut through the intensity distribution parallel to Q_x was used to determine $\delta q_x(|\mathbf{Q}_0|)$, while $\delta q_y(|\mathbf{Q}_0|)$ was obtained by a cut perpendicular to Q_x.

In the way described above and using the thick amorphous germanium layer on an Si wafer (Bloch, Brügemann & Press, 1989), the resolutions $\delta q_x(|\mathbf{Q}_0|)$ and $\delta q_y(|\mathbf{Q}_0|)$ were determined near the angle of total external reflection ($|\mathbf{Q}_0| = 0.0285$ Å^{-1}). Additional values for large $|\mathbf{Q}_0|$, here $|\mathbf{Q}_0| = 2.0038$ Å^{-1} and $|\mathbf{Q}_0| = 4.6277$ Å^{-1} (Si 111 and 004 reflection), also were measured. Fig. 2 shows the calculated (solid line) and measured (triangles and circles) values for δq_x and δq_y. We find an acceptable agreement between the calculations following Cowley's treatment and the measurements, especially in the case of a TCD with Si 111 crystals. Near $|\mathbf{Q}_0| = 0$ there is less agreement, but the condition $|\Delta\mathbf{Q}| \ll |\mathbf{Q}_0|$ is no longer fulfilled. For the asymmetric diffractometer configuration with Ge 111 and 311 crystals, the agreement is rather good. But in this case the matrix element M_{12} [see (2)] does not vanish, so that the calculated values for δq_x and δq_y represent lower limits for the resolution.

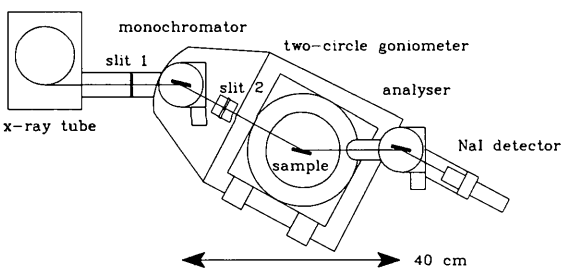

Fig. 1. Schematic drawing of the three-crystal diffractometers (plan view). In one case an Si(111) monochromator and analyser were used [symmetrical nondispersive Si(111)$^+$-sample$^-$-Si(111)$^+$ configuration]. The other configuration was an asymmetrical nondispersive set-up with Ge(111) monochromator and Ge(311) analyser.

As an example, Fig. 3 shows typical measured intensities in the vicinity of the Si 111 reciprocal-lattice point ($|\mathbf{Q}_0| = |\mathbf{G}_{111}| = 2.0038$ Å^{-1}) for the Si 111 TCD parallel and perpendicular to **G**. Fits of a Gaussian show good agreement. For greater departures from the exact Bragg position along ΔQ_x a discrepancy between calculation and measurement becomes visible. The reason for this is the CTR (Robinson, 1986), which is badly reproduced by a Gaussian fit.

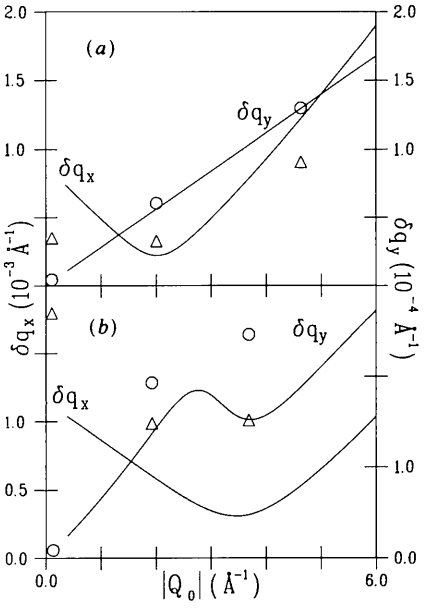

Fig. 2. The calculated resolution (solid line) parallel (δq_x) and perpendicular (δq_y) to $\mathbf{Q}_0$ as a function of $|\mathbf{Q}_0|$ for two types of three-crystal diffractometer. (*a*) represents the symmetrical silicon configuration and (*b*) represents the asymmetrical germanium configuration. The resolution values obtained by measurements are also plotted: circles correspond to δq_y, triangles to δq_x.

In Fig. 4 the intensity distribution around the Si 111 reflection for the nondispersive $Si(111)^+$-$Si(111)^-$-$Si(111)^+$ configuration (see Fig. 1) is shown. This is a configuration ideally suited to high-resolution X-ray scattering experiments. The isointensity contours were measured by rotating the scattering vector **Q** transversely through the reciprocal lattice for several values of $|\mathbf{Q}|$. Fig. 4 is composed of 41 rocking curves. The expected star-like intensity distribution is demonstrated on a logarithmic scale. The intensity streak parallel to ΔQ_x with $\Delta Q_y = 0$ is caused by the surface of the sample truncating its crystal lattice (CTR) and the other two streaks are the CTRs of the perfect monochromator and analyser. Their reflections give rise to Darwin-shape-like intensity streaks perpendicular to $\mathbf{k}_i$ and $\mathbf{k}_f$. Since the tilt angles of $\mathbf{k}_i$ and $\mathbf{k}_f$ are $\pm(90° - \Theta_{\text{Bragg}})$ with respect to **Q**, the streaks of the monochromator and analyser appear with a tilt angle of $\pm\Theta_{\text{Bragg}}$. If monolithic grooved crystals with multiple reflections are used, the CTRs of the monochromator and analyser streaks will be strongly suppressed (Iida & Kohra, 1979; Zaumseil & Winter, 1982).

Simultaneously with the star-like intensity distribution, the thermal diffuse scattering around the reciprocal-lattice point is visible but the intensity is several orders of magnitude weaker than that of the three streaks.

To calculate the intensity distribution, we assumed CTRs for the monochromator and analyser Si 111 reflections, the CTR of the Si 111 sample reflection along ΔQ_x and a ΔQ_y^{-4}-dependence of the intensity perpendicular to the CTR. For the region of total reflection the above-mentioned Darwin widths were used. The thermal diffuse scattering was neglected

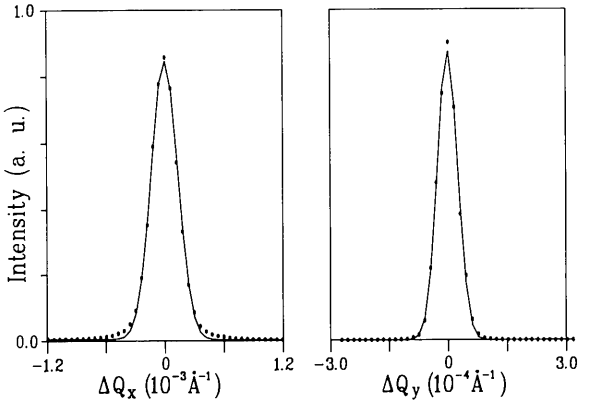

Fig. 3. The measured (dots) and fitted (line) resolution parallel (left) and perpendicular (right) to $\mathbf{Q}_0 = \mathbf{G}_{111}$. The data were obtained with the three-crystal diffractometer using the symmetrical nondispersive $Si(111)^+$-$Si(111)^-$-$Si(111)^+$ configuration. ΔQ_x and ΔQ_y are the components of the deviations of the scattering vector **Q** from the reciprocal-lattice point $\mathbf{G}_{111}$.

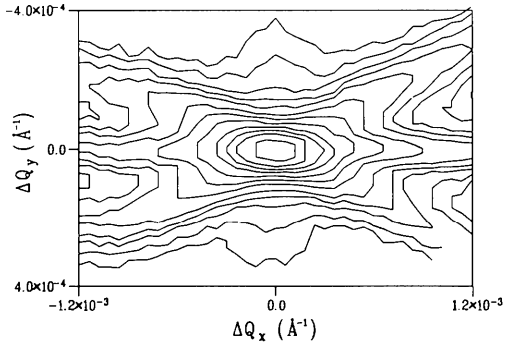

Fig. 4. The intensity distribution close to the silicon 111 reciprocal-lattice point obtained with the three-crystal diffractometer using silicon crystals. The lines represent $I/I_0 = 0.5, 0.2, 0.1, 0.05, \ldots$ with the maximum intensity I_0. ΔQ_x and ΔQ_y are the components of the deviations of the scattering vector **Q** from the reciprocal-lattice point $\mathbf{G}_{111}$ parallel and perpendicular to the [111] and the [11$\bar{2}$] directions. (For further information see text.)

and the vertical resolution was treated as completely decoupled.

Recognizing a different intensity decrease for the monochromator and analyser streak, we considered a reflection profile of the monochromator slightly different from the ideal CTR. The modified reflectivity can be caused by the white X-ray beam to which the monochromator crystal was exposed. This might result in a stronger oxidation (roughness) of the monochromator or it might cause defects in the surface region. We took this into account by allowing an exponent $r \geq 2$ for ΔQ^{-r} intensity decrease of the monochromator CTR (see also Robinson, 1986).

Fig. 5 shows the results of the calculation corresponding to the measurements shown in Fig. 4. Good agreement is achieved by using $r = 2.2$ for the above-mentioned intensity decrease of the monochromator reflection.

Bearing in mind that this calculation is capable of simulating the resolution effects of a TCD in an intensity range of four orders of magnitude, we can also interpret data obtained very close to reciprocal-lattice points. This is very interesting with regard to investigations of artificial and natural lattices with periodicities both parallel and perpendicular to the surface of single crystals with lattice parameters in the region of 10 Å [Burandt, Komorek, Schnabel, Press & Boysen (1992): density modulation crosswise through the lattice; Tolan, König, Brügemann, Press, Brinkop & Kotthaus, (1992): laterally structured surfaces].

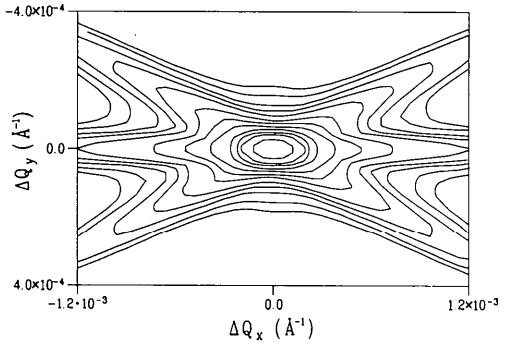

Fig. 5. The intensity distribution close to the silicon 111 reciprocal-lattice point calculated as described in the text. The lines represent an intensity relation $I/I_0 = 0.5, 0.2, 0.1, 0.05, \ldots$ with the intensity I_0 at the reciprocal-lattice point. ΔQ_x and ΔQ_y are the components of the deviations of the scattering vector **Q** from the reciprocal-lattice point $\mathbf{G}_{111}$.

4. Concluding remarks

The given comparison of measured and calculated resolution effects of three-crystal diffractometers using perfect crystals as monochromator and analyser shows very good agreement. This is valid for both investigated types of TCDs (symmetrical Si 111 and asymmetrical Ge 111 and 311 reflections, respectively). The agreement is reached both for the central part of the resolution function using an approach given by Cowley and the star-like resoution near a reciprocal-lattice point. The latter was calculated following the dynamical description of the TCD suggested by Pinsker.

The intensity distribution close to a reciprocal-lattice point shows the predicted star-like shape caused by the overlap of the diffraction by the perfect sample and the reflection curves of the perfect monochromator and analyser crystals. A difference in the reflectivity shape of the monochromator and analyser is identified as an intensity decrease due to oxidation effects or near-surface defects caused by the white X-ray beam the first crystal of a TCD is exposed to.

This work was supported by the Bundesministerium für Forschung und Technologie under contract no. 05 401 AB12. The authors thank D. Bahr for helpful discussions.

References

BLOCH, R., BAHR, D., OLDE, J., BRÜGEMANN, L. & PRESS, W. (1990). *Phys. Rev. B*, **42**, 5093-5099.

BLOCH, R., BRÜGEMANN, L. & PRESS, W. (1989). *J. Phys. D*, **22**, 1136-1142.

BRÜGEMANN, L., BLOCH, R., PRESS, W. & GERLACH, P. (1990). *J. Phys. Condens. Matter*, **2**, 8869-8879.

BURANDT, B., KOMOREK, M., SCHNABEL, B., PRESS, W. & BOYSEN, H. (1992). *Z. Kristallogr. Kristallgeom. Kristallphys. Kristallchem.* In the press.

CHESSER, N. J. & AXE, J. D. (1973). *Acta Cryst.* A**29**, 160-169.

COOPER, M. J. & NATHANS, R. (1967). *Acta Cryst.* **23**, 357-367.

COWLEY, R. A. (1987). *Acta Cryst.* A**43**, 825-836.

GRIMM, H. (1984). *Nucl. Instrum. Methods*, **216**, 553-557.

IIDA, A. & KOHRA, K. (1979). *Phys. Status Solidi A*, **51**, 533-542.

PINSKER, Z. G. (1978). *Dynamical Scattering of X-rays in Crystals. Springer Series in Solid State Science* 3. Berlin: Springer.

PYNN, R., FUJII, Y. & SHIRANE, G. (1983). *Acta Cryst.* A**39**, 38-46.

ROBINSON, I. K. (1986). *Phys. Rev. B*, **33**, 3830-3836.

ROBINSON, I. K., WASKIEWICZ, W. K., TUNG, R. T. & BOHR, J. (1986). *Phys. Rev. Lett.* **57**, 2714-2717.

RYAN, T. W. (1986). PhD thesis, Edinburgh Univ., Scotland.

RYAN, T. W., HATTON, P. D., BATES, S., WATT, M., SOTOMEYER-TORRES, C., CLAXTON, P. & ROBERTS, J. S. (1987). *Semicond. Sci. Technol.* **2**, 241-243.

TOLAN, M., KÖNIG, G., BRÜGEMANN, L., PRESS, W., BRINKOP, F. & KOTTHAUS, J. P. (1992). *Europhys. Lett.* Submitted.

ZAUMSEIL, P. & WINTER, U. (1982). *Phys. Status Solidi A*, **70**, 497-505.